
Article:
Otitoju, O., Oko, E. and Wang, M. orcid.org/0000-0001-9752-270X (2021) Technical and economic performance assessment of post-combustion carbon capture using piperazine for large scale natural gas combined cycle power plants through process simulation. Applied Energy, 292. 116893. ISSN 0306-2619

https://doi.org/10.1016/j.apenergy.2021.116893

Technical and economic performance assessment of post-combustion carbon capture using piperazine for large scale natural gas combined cycle power plants through process simulation

Olajide Otitoju[a], Eni Oko[b], Meihong Wang[a]*

[a]Department of Chemical and Biological Engineering, University of Sheffield, Sheffield S1 3JD,

[b]Department of Chemical Engineering, University of Hull. HU6 7RX

*Corresponding author: Tel: +44(0)114 – 222–7160. E-mail: Meihong.Wang@sheffield.ac.uk,

Abstract

The main challenges to the commercial deployment of the solvent-based post-combustion carbon capture technology include high energy consumption and high capital and operating costs. New solvents and alternative process configurations are being pursued to reduce the energy consumption and costs of the process. This paper investigates the technical and economic performance of the process using piperazine (PZ) solvent for a 250 MW_e natural gas combined cycle power plant. Three different configurations of the process using PZ were evaluated and compared to the standard process using 30 wt% monoethanolamine (MEA) solvent. The technical performance of the process was evaluated using the rate-based model developed in Aspen Plus® V8.4 and the economic evaluation was carried out in Aspen Process Economic Analyzer®V8.4. The technical results showed that the total energy demand of the process reduces from 5.34 GJ/t_{CO2} using 30 wt% MEA to 3.56 GJ/t_{CO2} using 30 wt% PZ. The lowest energy demand of 2.76 GJ/t_{CO2} was achieved with the advanced flash stripper using 40 wt% PZ. The economic results show that the lowest total annual cost of M$26.58 per year and CO_2 capture cost of $34.65 per $tonne_{CO2}$ were obtained using the advanced flash stripper (AFS) with 40 wt% PZ. It was concluded that the 40 wt% PZ solvent would bring practical technical and economic benefits to the large-scale applications of the capture process compared to the current 30 wt% MEA solution. Therefore, this study will inspire policymakers and researchers towards the large-scale deployment of solvent-based PCC process.

Keywords: *Post-combustion carbon capture (PCC); Chemical absorption; piperazine; technical and economic evaluation; natural gas combined cycle power plant; advanced flash stripper.*

Nomenclature

C_i	Molarity of component *i* (kmol/m^3)
E_j	Activation energy (kJ/kmol)
K_{eq}	Equilibrium constant
k_j^o	Pre-exponential factor for reaction j (m^3/kmol.s)
R	Universal gas constant (kJ/kmol K)
k_r	Reaction rate (m^3/kmol.s)
T	Temperature (K)
W_{comp}	Compression work (GJ/t_{CO2})
W_{eq}	Total equivalent work (GJ/t_{CO2})
W_{pump}	Pump work (GJ/t_{CO2})

Abbreviations

ACC	Annual capital cost
AFS	Advanced flash stripper
APEA	Aspen Process Economic Analyser®
NGCC	Natural gas combined-cycle
PCC	Post-combustion carbon capture

1. Introduction

1.1. Background

The need to reduce CO_2 emission from flue gases of fossil-fuel-fired power plants and move towards a CO_2 neutral energy market have intensified the efforts to integrate the power plants with carbon capture and sequestration technologies. Fossil-fuel-fired power plants such as NGCC are the single largest source of CO_2 emissions which is responsible for climate change[1]. An unabated NGCC power plant emits about 450 kg of CO_2 per Megawatt-hour of electricity [2,3]. This is less than half the amount of CO_2 released per unit of electricity generated from a coal-fired power plant [3]. While the transition to renewable energy is ongoing albeit, at a rather slow pace, post-combustion carbon capture (PCC) via chemical absorption has been identified as the most promising and matured carbon capture technology for short and mid-term decarbonisation of the energy sector [4]. However, the parasitic energy demand and the high cost of the PCC process are the main hindrances to the speedy and extensive deployment of the PCC technology on a large-scale [5].

One possible route to the energy-efficient CO_2 capture process is the use of alternative chemical solvents such as piperazine with high CO_2 loading capacity and low regeneration energy. Piperazine is a cyclic diamine consisting of six-membered saturated rings. It is an effective rate promoter and it is capable of absorbing 2 moles of CO_2 per mole of amine theoretically. Pilot plant experimental studies have shown that about 10-20% reduction in energy requirement of the PCC process can be achieved with piperazine as solvent [6].

1.2. Literature review

Absorption of CO_2 with the benchmark solvent of 30 wt% MEA has been investigated by several researchers [7–11]. MEA is highly corrosive, volatile, and degrades rapidly at temperatures above 120 °C, and by pollutants such as NO_X, O_2, and SO_2. Despite implementing several process configurations such as heat integration, vapour re-compression, multi-pressure configuration, split flow regime, absorber intercooling, selective exhaust gas recirculation and the addition of auxiliary equipment like heat pumps [2,10,12–16] the energy required by the capture process with MEA is still high (3.3-5 GJ/ton_{CO2}). Specifically, an MEA-based capture process installed in an NGCC power plant would impose a thermal efficiency penalty of between 7-13% [2,7,17] which could lead to an increase in the cost of electricity.

In the past, PZ has been mostly used in blends as a promoter in tertiary amines and carbonate solutions [18]. At present, it has been established that it can be used as a single solvent in the PCC process [19]. Aqueous piperazine solution has also been proposed in the literature as an alternative solvent to MEA for the PCC process [20]. It has been demonstrated to have lower volatility, higher CO_2 absorption capacity, twice the absorption rate of 30 wt% MEA and higher resistance to oxidative and thermal degradation [21]. It was also reported to have good heat transfer properties that resulted in a higher normalized capacity of 27% above 30 wt% MEA [22]. Therefore, PZ is chosen as the solvent in this study because of its superior properties to MEA. Table 1 shows the performance parameter of 40 wt% PZ compared to 30 wt% MEA. The limitation of PZ as a solvent in PCC is related to solid formation in lean solution at temperatures below 20 °C. Piperazine hydrate (PZ·6H2O(s)) precipitates out of solution at low CO_2 loadings and could lead to the formation of solid in the lean solvent [23]. Therefore, care must be taken during plant start-up, operation and shutdown.

Table 1. Performance parameters of 30 wt% MEA versus 40 wt% PZ

Parameter	30 wt% MEA	40 wt% PZ	Source
K_L @40 °C (mol/s.Pa.m^2)	4.3 x 10^{-7}	8.5 x 10^{-7}	[21]
Viscosity (Pa.s) @ 40 ^{0}C	0.003	0.011	[21]
CO_2 Capacity (mol_{CO2} /mol_{amine})	0.5	0.79	[24]
Heat of absorption (kJ/mol_{CO2})	85	75	[25,26]
Oxidative degradation @ 55 °C (mmol amine/kg-hr)	12	1.1	[20]
Thermal degradation (Amine loss at 150 °C in % per week)	11	0.44	[20]
Thermal stability T_{max} (°C)	120	163	[27]
Max. regeneration Pressures (bar)	2.2	14	[21]
Volatility at lean loading, @ 40 °C (ppm)	31	8	[28]

The 40 wt% PZ is considered as the standard solvent concentration for the PCC process with PZ. CO_2 absorption with PZ has been extensively studied at pilot plant facilities such as the J.J pickle facility at the University of Texas at Austin, USA [21,29,30], the CO_2 SEParation PLant (CO2SEPPL) at the EVN power plant in Dürnrohr, Austria [23,31], the CSIRO CO_2 capture pilot plant at Tarong power plant in Queensland, Australia [32], and the National Carbon Capture gas Centre (NCCC) in Wilsonville, Alabama, USA [6,22,33]. The findings from the CO2SEPPL at the EVN power plant in Austria show that the regeneration energy of the PCC process can be reduced by 14% using 37.5 wt% PZ. The CSIRO capture plant at Tarong power plant found the lowest regeneration energy of 2.9 GJ/t_{CO2} using 40 wt% PZ, this is 15% lower than the regeneration energy obtained using 30 wt% MEA in the same pilot plant. Pilot plant studies [6,33] at the NCCC have been exploring the energy performance benefits of 30 wt% PZ with process modifications including absorber intercooling and the advanced flash stripper (AFS). Results have demonstrated that the regeneration energy of between 1.9 and 2.5 GJ/t_{CO2} could be achieved for a CO_2 capture level of between 83 and 99% from the flue gas of a coal-fired power plant.

Other studies have explored the operational benefits of different process configurations for CO_2 capture with PZ. For instance, the operational benefits of the different absorber (adiabatic, in-and-out, and pump-around intercooling) and stripper (simple, two-stage flash and advanced flash) configurations have been quantified for CO_2 capture with PZ from coal-fired power plants [26]. Absorber intercooling improves the absorption process by reducing the temperature bulge, increase the solvent capacity and driving force, consequently reducing the packing and regeneration energy requirements. Plaza and Rochelle [29] reported a 10% increase in CO_2 capture with PZ in an intercooled absorber operated with flue gas with 13 mol% CO_2.

Madan et al**.** [34] optimized the energy performance of the CO_2 stripping process in a two-stage flash stripper and found an 11% improvement in the equivalent work of the process compared to operation with the standard stripper. This result was achieved by assuming a specific set of optimized conditions including rich loading of 0.4 mol_{CO2}/mol_{PZ}, lean loading of 0.31 mol_{CO2}/mol_{PZ}, and 4% bypass flow. In more recent tests using the AFS with cold and warm rich solvent bypass, a 25% less energy demand was achieved compared to the two-stage flash stripper [35].

Although the energy consumption is important when discussing the improvements achieved through these alternative process configurations, it is however not the only parameter to assess and rank the performance of these configurations. For instance, most of the alternative configurations require extra equipment such as heat exchangers and pumps that would add to the

capital investment of the process. The economic implication of such additions needs to be ascertained to be sure the extra capital investment would not offset the energy gain achieved through these alternative process configurations. An economic evaluation of these process configurations using the total annual cost and a more rigorous index such as the "cost of CO_2 capture" provides a more robust and objective assessment. The cost of CO_2 capture takes into account both the energy performance and the capital, operating, and maintenance costs of the process and has been used by different researchers to assessed and rank different configurations of the capture processes [36–38]. Therefore, the economic performance of the configurations considered in this work is assessed using the total annual costs and the cost of CO_2 captured.

1.3. Novelty

Several studies with a focus on the technical and economic analysis of the PCC process using MEA have been carried out [9,37,39,40], and are available in the literature. Fundamental to these studies are reliable, closed-loop models of the process. Previous modelling and simulation of the PCC process using PZ focused on model development and model validation of the standalone absorber [41–43] and the standalone stripper [34,35]. Although these standalone (open loop) models are useful in identifying key process parameters and performance trends, the communication between process units tends to be unidirectional (without recycle) and as such does not give a realistic prediction of the PCC process. Considering that the PCC process in real life is in a closed-loop, therefore, a closed-loop model would be required to accurately predict its behaviour. The closed-loop model considers the many interacting unit operations and variables of the PCC process thereby resulting in more accurate predictions of process performance and costs. Additionally, closed-loop models are critical when identifying the global optimal set of operating parameters. The closed-loop model of the PCC process using PZ has not been reported in literature. In this study, a closed-loop model of the PCC capture process using PZ has been developed for the first time and validated at pilot scale with experimental data. This was followed by scale-up of the pilot-scale capture model to a large-scale capture model for a 250MW_e NGCC power plant.

Previous modelling and simulation studies with PZ solvent focussed on CO_2 capture from coal-fired power plants [29,44,45]. However, due to the increasing use of NGCC power plants for electricity generation, most of the new fossil-fuel-fired power plants addition would be NGCC, it is therefore imperative to design and study the possible requirements of a large-scale PCC plant for an NGCC application using PZ as a solvent. The technical assessment of the PCC process using different process configurations and different concentrations of PZ is yet to be demonstrated for large-scale NGCC power plants. In this work, the PCC plant for a 250 MW_e NGCC power plant has been designed and simulated in Aspen Plus® starting with the standard configuration of the process using PZ. In addition to this, two other configurations of the PCC process using PZ which represent different technical innovations (intercooling and AFS) were also simulated and analysed to assess their operational benefits in terms of energy consumption.

Furthermore, previous studies have not shown a detailed economic assessment of the large-scale PCC process using PZ for NGCC power plants. A detailed economic assessment of the PCC process normally involves the calculation of the capital expenditure, operating and maintenances cost, total annual cost and the cost of CO_2 capture. An economic evaluation of the PCC process with detailed calculation of these costs has not been reported for different configurations of the PZ-based PCC process treating flue gas from an NGCC power plant. Considering that cost is the most sensitive criterion when deciding on the commercial deployment of a new technology such as the PCC process using PZ, it is important to carry out a detailed economic assessment of the technology. This economic assessment will provide decision-makers with relevant information on the cost of the technology thereby aiding in their decision-making process. In this study, an economic evaluation of the different process configurations of the PCC process with different concentrations of PZ is carried out in Aspen Process Economic Analyser® (APEA). The combined

impacts of the process configurations and PZ concentrations on the capital expenditure (CAPEX), operating and maintenance expenditure (OPEX), total annual cost and the cost of CO_2 captured were evaluated.

2. Process description

2.1. Standard PCC process using PZ

The process configuration of the standard PCC process using PZ is shown in Figure 1. It consists of the absorber, stripper, pumps, heat exchangers and a compression unit. The PCC process is designed to capture 90% of the CO_2 in the flue gas and to attain >95% purity for the CO_2 product. The captured CO_2 is compressed to 150 bar for transportation and geological storage sites. Other configurations are compared to the standard process using PZ.

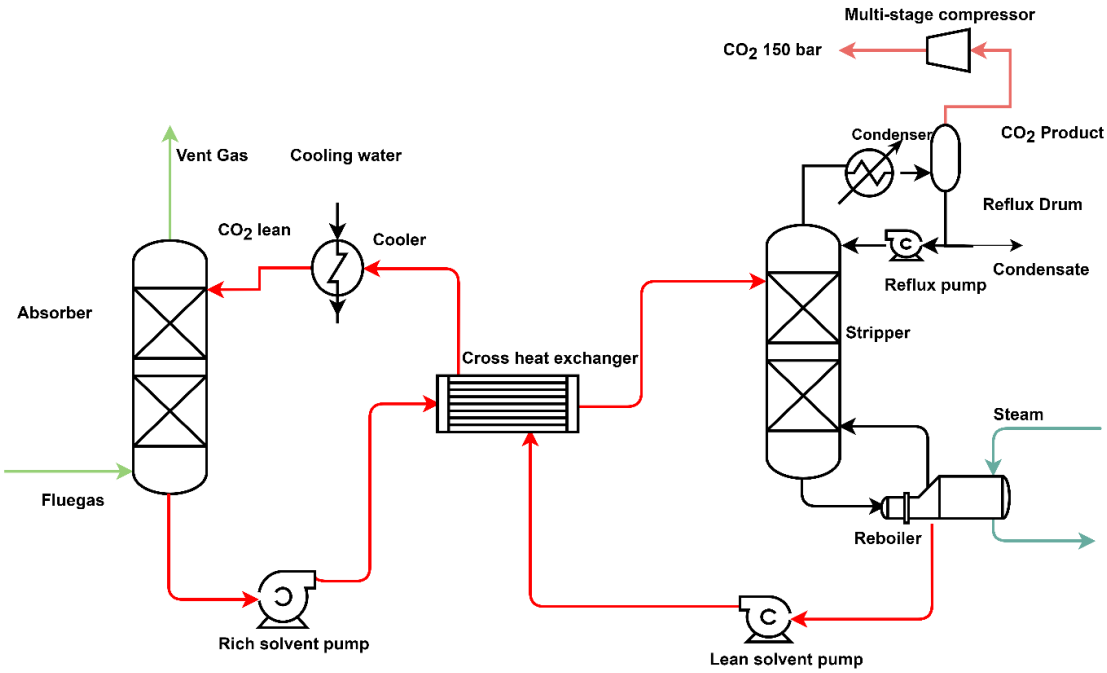

Fig. 1. Standard PCC process configurations using PZ [1]

2.2. Absorber intercooling

A variant of the standard process configuration created by adding an absorber intercooler and a pump is shown in Fig.2. Due to the low CO_2 concentration in the flue gas from an NGCC power plant, a low L/G ratio is often required for CO_2 absorption. Therefore, during absorption, the solvent temperature in the absorber increases thereby reducing the solvent absorption capacity. Intercooling is often used to cool the solvent. Intercooling reduces the liquid phase temperature in the absorber thereby lowering the equilibrium CO_2 partial pressure. This increases the potential for mass transfer and therefore enhances the cyclic capacity of the solvent. This could potentially reduce the required packing height and the energy requirement for solvent regeneration.

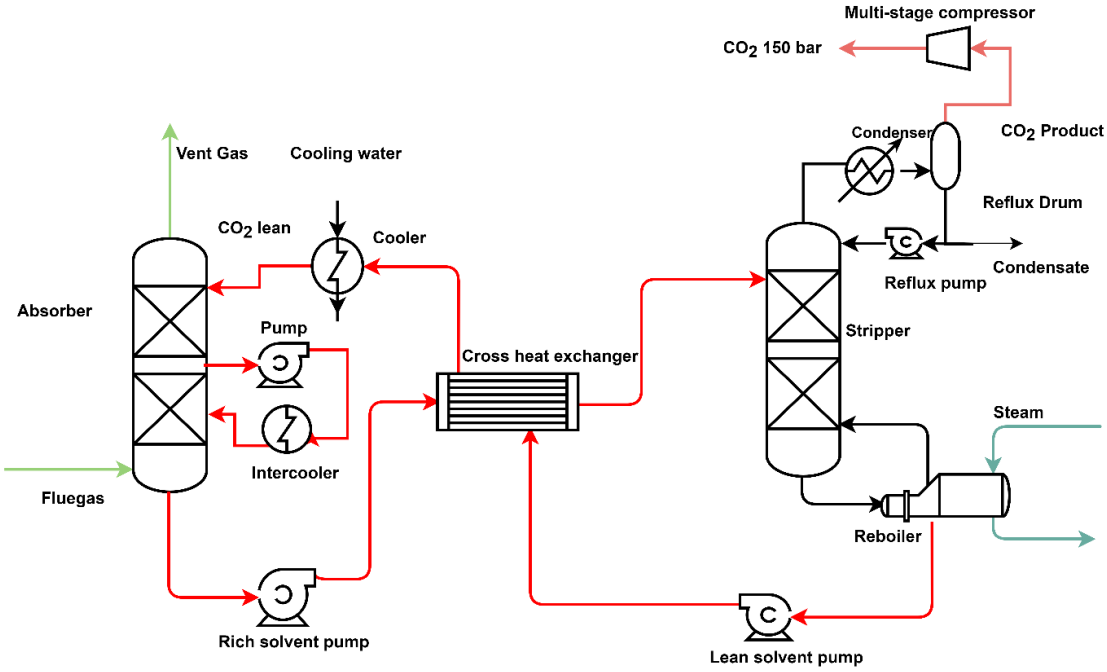

Fig. 2 Absorber intercooling in the PCC process using PZ [46]

2.3. Advanced flash stripper (AFS)

The AFS with cold and warm rich bypass was proposed and tested at pilot scale [35]. A schematic of the AFS is shown in Fig.3. Unlike the standard configuration, the cross-heat exchanger in the AFS is split into two (cold and hot cross-exchangers). The rich solvent exiting the absorber was pumped through the rich solvent pump to raise the pressure to the stripper pressure. This solvent was pre-heated by the lean solvent from the stripper before being split into cold-rich and warm-rich bypass before and after the cold cross-exchanger. The cold-rich bypass was heated by the hot vapour exiting the top of the stripper. It was then mixed with the warm rich bypass before being fed to the top of the stripper. Due to the colder temperature of this bypass stream compared to the top feed of a standard stripper, the energy performance is enhanced by recovering latent heat and condensing water vapour. The rest of the steam exiting the hot-cross exchanger was further heated in a steam heater before being fed to the flash tank at the bottom of the stripper. The steam heater and the flash tank functioned as the reboiler in contrast to the reboiler in the standard stripper.

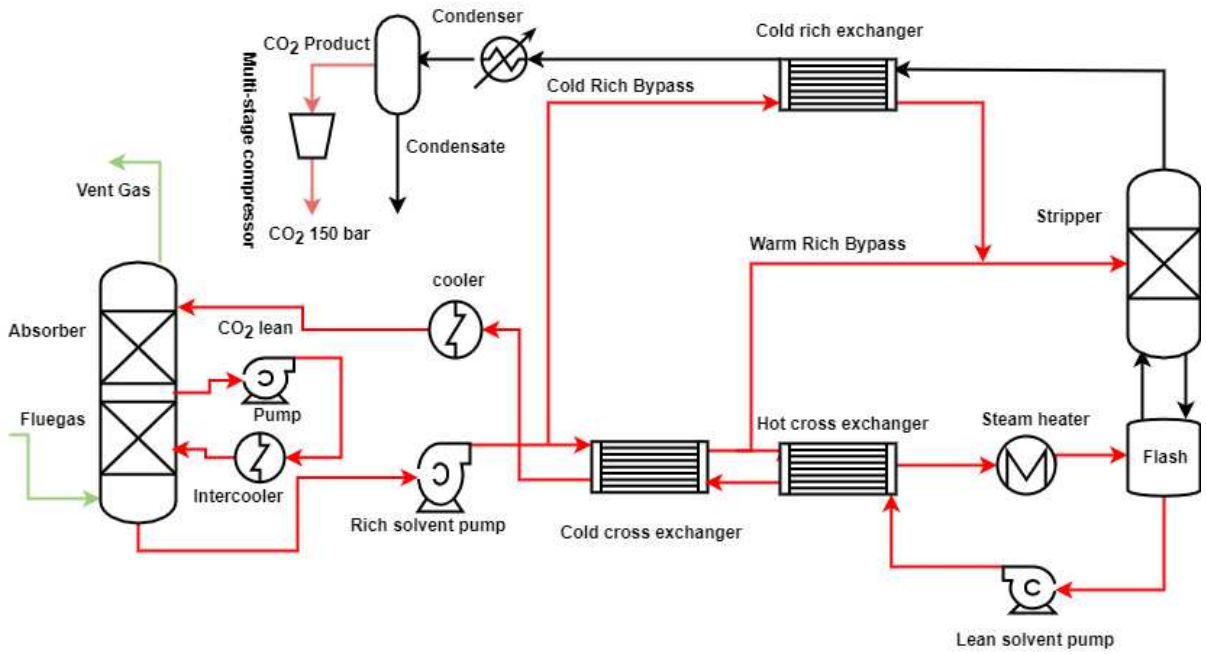

Fig. 3 Advanced flash stripper in the PCC process using PZ [35]

3. Methodology

3.1. Model development

The model of the PCC process using PZ was developed in Aspen Plus® V8.4 using the rate-based model approach. The model includes electrolyte chemistry, column hydrodynamics and detailed component mass transfer calculations between phases. Furthermore, the rate-based model includes correlations for calculating the thermodynamic, kinetic and physical properties as well as models for the rigorous unit operations of the absorber and stripper. The liquid phase non-ideality was calculated with the Electrolyte Non-Random Two-Liquid (ElecNRTL) thermodynamic method and that of the vapour phase was computed with the Redlich-Kwong equation of state. The chemistry of CO_2 absorption with aqueous PZ is described by the set of equilibrium reactions presented in Eqs. 1 – 7 [47].

$$2H_2O \rightleftarrows H_3O^+ + OH^- \quad (1)$$

$$CO_2 + 2H_2O \rightleftarrows HCO_3^- + H_3O^+ \quad (2)$$

$$H_2O + HCO_3^- \rightleftarrows CO_3^{2-} + H_3O^+ \quad (3)$$

$$PZH^+ + H_2O \rightleftarrows PZ + H_3O^+ \quad (4)$$

$$PZ + HCO_3^- \rightleftarrows PZCOO^- + H_2O \quad (5)$$

$$H^+PZCOO^- + H_2O \rightleftarrows PZCOO^- + H_3O^+ \quad (6)$$

$$PZCOO^- + HCO_3^- \rightleftarrows PZ(COO^-)_2 + H_2O \quad (7)$$

The temperature-dependent equilibrium constants (K_{eq}) for these reactions are defined on a molar concentration scale and have been determined from the following expression:

$$\ln K_{eq} = A + \frac{B}{T} + C \ln T + DT \quad (8)$$

The chemical reactions depicted in Eqs. 1- 3 represent the dissociations of water, the formation of bicarbonate and the formation of carbonate. The coefficients of the equilibrium constant for these reactions (Eq. 8) were taken from Posey and Rochelle [48]. The reaction in Eq 4 represents the protonation of PZ and the coefficients for calculating the equilibrium constant were obtained from Hetzer et al. [49]. The reactions in Eqs. 5-7 involve carbamated PZ species (i.e formation of piperazine monocarbamate (Eq. 5), dissociation of protonated carbamate zwitterion (Eq. 6) and formation of piperazine dicarbamate (Eq. 8)). The coefficients of the equilibrium constant for these reactions were obtained from Ermatchkov et al. [50].

The reactions shown in Eqs. 9-14 are kinetically controlled. These sets of reactions control the rate of absorption and enhance mass transfer from the gas phase to the liquid phase.

$$CO_2 + OH^- \rightarrow HCO_3^- \quad (9)$$

$$HCO_3^- \rightarrow CO_2 + OH^- \quad (10)$$

$$PZ + CO_2 + H_2O \rightarrow PZCOO^- + H_3O^+ \quad (11)$$

$$PZCOO^- + H_3O^+ \rightarrow PZ + CO_2 + H_2O \quad (12)$$

$$PZCOO^- + CO_2 + H_2O \rightarrow PZ(COO^-)_2 + H_3O^+ \quad (13)$$

$$PZ(COO^-)_2 + H_3O^+ \rightarrow PZCOO^- + CO_2 + H_2O \quad (14)$$

The reaction rates (k_j) of the kinetic reactions (9-14) are determined using the power-law expressed as follows:

$$k_j = k_j^o \, exp\left(-\frac{E_j}{RT}\right) \prod_{i=1}^{N} C_i^{aij} \quad (15)$$

Where k_j^o is the pre-exponential factor, E_j is the activation energy, T is the system temperature, R is the universal gas constant, C_i is the concentration of species i, aij is the reaction order of component *i* in reaction *j*. Kinetic parameters used in the power-law to calculate the reaction rate of reactions 9-11 are presented in Table 2.

Table 2. Kinetic parameter for the rate-controlled reactions (Eqs. 9-14) [51,52]

Reaction No.	k_j^o $(m^3/kmol.s)$	E_j (kJ/kmol)
9	4.32e+13	5.55e+4
10	2.38e+17	1.23e+5
11	4.14e+10	3.36e+4
12	7.94e+21	6.59e+4
13	3.62e+10	3.36e+4
14	5.56e+25	7.69e+4

The absorber and the stripper were configured to have 20 stages each. The bulk properties which contribute to the calculation of reaction rates, mass and energy fluxes were modelled with the counter-current flow model. This flow model closely approximates the flow in the packed column and calculates the bulk properties of the phases as an average of the inlet and outlet conditions [53]. Since the reactions between PZ and CO_2 occur very fast and take place in the liquid phase

only, the "Discrxn" option which considers diffusion resistance with reactions in the film was chosen for the liquid phase and the "Film" option which considers diffusion resistance but no reaction in the film was specified for the gas phase. Additionally, the liquid film was discretized into 10 small segments.

Relevant correlations for predicting the thermo-physical properties of the liquid and vapour phases namely density, viscosity, diffusivity, surface tension, and thermal conductivity were also included in the model. The density of the liquid mixture was obtained by the Rackett model [54] and that of the gas phase was calculated by the Redlich Kwong equation of state [55]. The Jones-dole electrolyte model [56] was applied to compute the viscosity of the liquid mixture while the Chapman-Enskog model [57] was used to calculate the viscosity of the vapour mixture. The diffusivity of CO_2 in water and PZ solution was calculated with the Wilke-Chang model [58] and the Hakim-Steinberg-Stiel equation with Onsager-Samaras electrolyte correction [56] was used to obtain the surface tension of the liquid mixture. The thermal conductivity of the liquid mixture was estimated using the Riedel thermal conductivity model and that of the vapour mixture was computed using the Wassiljewa-Mason-Saxena model [59]. The mass transfer coefficient and the interfacial area are obtained from Hanley and Chen [60] correlation for structured packing. The heat transfer coefficient is estimated based on the Chilton-Colburn analogy [61] and the liquid holdup at each finite volume of packing was calculated by the correlation of Bravo et al. [62].

3.2. Model validation

To test the performance of the steady-state rate-based model described in section 3.1, 14 experimental cases reported by Rochelle and Plaza [29] for the absorber and by Van Wagener [63] for the stripper in a pilot plant campaign were simulated. The experiments were conducted at the CO_2 capture facility located at the J.J Pickle Research Centre and operated under the Separation Research Programme at the University of Texas at Austin, USA. The absorber and the stripper of the pilot plant each have a diameter of 0.427 m and each consists of two 3.05 m sections packed with Mellapak 2X. All the 14 experimental runs were carried out using a synthetic flue gas of constant volumetric flow rate (0.165 m^3/s) and CO_2 content of 12 mol%. The flue gas was contacted with PZ solution of varying concentrations (28.50 wt% PZ-44.05 wt% PZ). The range of the key operating parameters are summarized in Table 3 while details of the pilot plant campaign and the main operating conditions of the absorber and the stripper can be found in Plaza and Rochelle [29] and Van Wagener [63] respectively.

Table 3. Summary of the operating conditions for the PZ-based PCC pilot plant [29,63]

Operating conditions	Value
CO_2 in the flue gas (mol%)	12
Flue gas temperature (K)	281.15-294.15
PZ concentration (wt%)	28.50-44.05
Lean solvent flow (kg/s)	0.81-1.28
L/G ratio (mol/mol)	4.80-7.10
Capture level (%)	32.00-92.20
Absorber pressure (bar)	1.01
Stripper pressure (bar)	1.38-4.14
Reboiler temperature (K)	360.15-402.15
Condenser temperature (K)	277.95-298.35
Stripped CO_2 rate (kg/hr)	39.60-129.60
Specific reboiler duty (MJ/kg_{CO2})	3.88-4.59
Lean loading (mol_{CO2}/mol_{PZ})	0.25-0.33

The results of the rate-based model predictions against experimental measurements for CO_2 capture level, rich CO_2 loading and reboiler duty are shown in Figs. 4-6. It can be generally concluded that the model satisfactorily predicted the comprehensive pilot-plant results as deviations between model predictions and pilot-plant results are generally within ±10. This good agreement demonstrates and justifies the reliability of the rate-based model. To demonstrates the superiority of the closed-loop model to the open-loop model, results obtained for the open-loop (standalone absorber and standalone stripper models) and closed-loop simulation based on CO_2 capture level, lean and rich CO_2 loadings, captured CO_2 rate and reboiler duty measured in the pilot plant for the two selected cases (3 and 5) are compared in Table A1 of the Appendix. Results showed that the closed-loop model gives a better prediction of the experimental data compared to the open-loop model. The relative errors are generally lower for the closed-loop model compared to the open-loop model. Furthermore, the average relative error of the closed-loop model is about 1% while that of the open-loop model is about 7%.

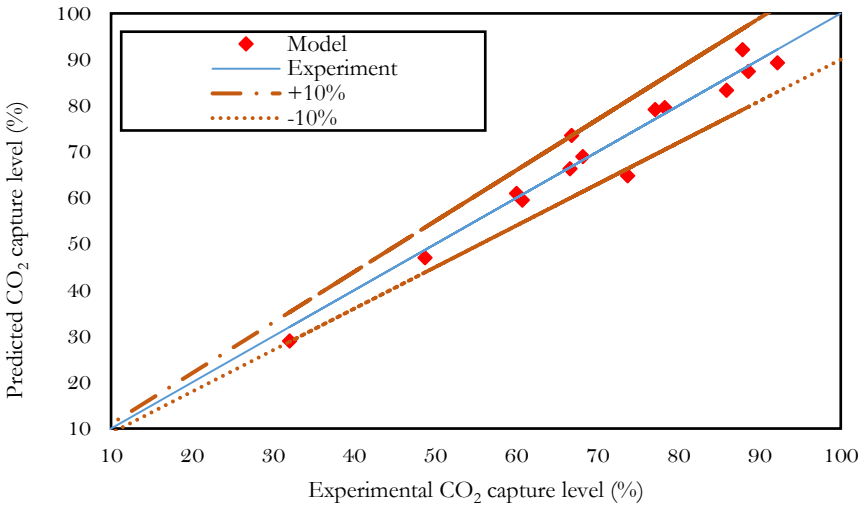

Fig. 4. Experimental data versus model prediction for CO_2 capture level for the 14 experimental cases (red diamond: model predictions; blue solid line: experimental data)

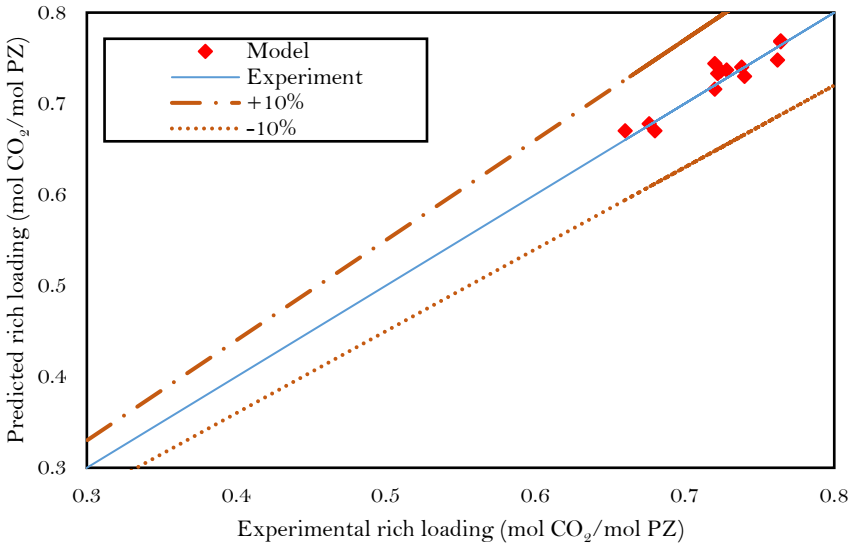

Fig.5. Experimental data versus model prediction for rich CO_2 loading for the 14 experimental cases (red diamond: model predictions; blue solid line: experimental data)

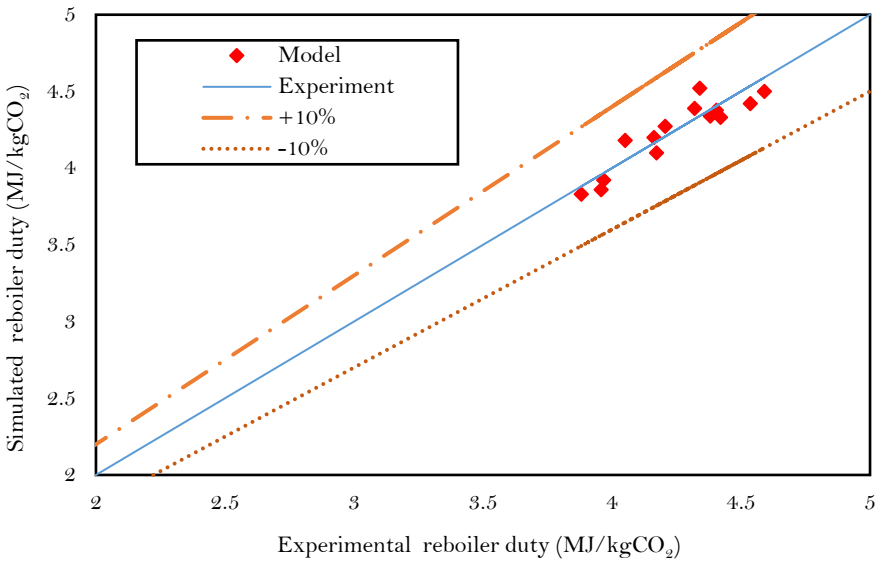

Fig. 6. Experimental data versus model prediction for specific reboiler duty for the 14 experimental cases (red diamond: model predictions; blue solid line: experimental data)

3.3. Model scale-up

The pilot-scale model developed in section 3.1 and validated in section 3.2 is scaled up to a PCC plant capable of capturing 90% of CO_2 in the flue gas from a 250 MW_e NGCC power plant. The flue gas conditions were exemplarily chosen as typical values for an NGCC power plant. The mass flow rate and temperature of the flue gas at the inlet to the absorber are 356 kg/s and 313 K respectively. It consists of CO_2 (4.90 mol%), N_2 (87.40 mol%), H_2O (6.63 mol%), and Ar (1.07 mol%) [7]. These conditions correspond to those specified by the case without exhaust gas recirculation (EGR). The required solvent flow rate to achieve 90% CO_2 capture at full-scale was estimated using the approach described by Agbonghae et al. [40]. The solvent absorption capacity from the pilot plant was adopted for large-scale calculations.

The diameter of the columns at full-scale was calculated following the scale-up approach described in Otitoju et al. [64] which involved calculating the diameter of the absorber and the stripper from flooding velocity. The values of quantities such as the densities of the liquid and the gas phases and the liquid viscosity used in the scale-up calculations were obtained from the pilot plant simulation. To prevent flooding in the columns, the flooding factor was set up to 70%. The diameter of the absorber and the stripper were determined to be approximately 12.5 m and 8 m respectively. The Mellapak 2X packing used in the pilot plant [29] is adopted for the large-scale PCC plant. The values of the diameter and packing height of the absorber and stripper used to simulate the standard configuration of the large-scale PCC process using PZ are shown in Table 4.

Table 4. Dimensions of the absorber and the stripper for the large-scale standard PCC process configuration

Standard PCC process configuration	
Absorber	
Diameter (m)	12.5
Packing height (m)	20
Packing type	Mellapak 2X
Stripper	
Diameter (m)	8
Packing height (m)	20
Packing type	Mellapak 2X

4. **Large-scale PCC process**

4.1 Simulation of the different configurations

In this section, the three process configurations of the PCC process using PZ described in section 2 are simulated. For each configuration, both the PZ concentration and the lean solvent CO_2 loading were varied. The PZ concentration was varied from 30 to 40 wt%. This is to avoid operational problems that are associated with high viscosity. As the concentration of PZ increases, the viscosity also increases. For instance, at 40 wt% the viscosity of PZ solvent is 0.011 Pa.s [21]. Beyond this concentration, the viscosity of the PZ solvent increased greatly (e.g. at 45 wt%, the viscosity of PZ solvent is 0.024 Pa.s [65] a 54% increase from the viscosity at 40 wt%). High viscosity would hinder solvent flow, decrease mass transfer in the exchangers and interferes with mass transfer. These would lead to an increase in process equipment (heat exchangers, pumps etc) size and eventually the cost of the PCC process. The lean solvent CO_2 loading was varied from 0.16 to 0.3 mol_{CO2}/mol_{PZ}. The stripper pressure was kept constant at 1.65 bar for all configurations. This resulted in changes in the temperature needed to achieve the desired CO_2 loading in the lean solvent at the bottom of the stripper. Although PZ has been reported to be resistant to thermal degradation at temperatures up to 423 K [66], a maximum temperature of 393 K was used in this study for solvent regeneration in the stripper. The flue gas flow rate, composition and temperature were kept constant for all cases.

Table 5. Process input parameters for the large-scale PZ-based PCC process

Parameters	Values
CO_2 capture level	90
PZ concentration (wt%)	30, 35, 40
Lean solvent temperature (K)	313.15
Rich solvent pump pressure (bar)	2.10
Lean solvent pump pressure (bar)	1.65
Cross heat exchanger Temperature approach (K)	10
Absorber pressure (bar)	1.01
Stripper pressure (bar)	1.65
Condenser temperature (K)	298.15

The standard configuration of the large-scale PCC process was first developed using input parameters in Tables 4 and 5. Later, the absorber was modified to include intercoolers. The pump-around intercooling was used in this work since it has been reported to perform better at NGCC conditions than in-and-out intercooling [33]. The intercooling was implemented in Aspen Plus®

by removing liquid from a lower stage, cooled to 35 °C and returned to an upper stage in the absorber. The values of the absorber and stripper diameters and the packing heights used to simulate the intercooled and the AFS configurations are shown in Table 6.

Table 6. Dimensions of the absorber and the stripper for the large-scale intercooled and AFS process configurations

	Intercooled configuration	Advanced flash stripper
Absorber		
Diameter (m)	12	12
Packing height (m)	15	15
Packing type	Mellapak 2X	Mellapak 2X
Stripper		
Diameter (m)	8	7.6
Packing height (m)	15	10
Packing type	Mellapak 2X	Mellapak 2X

The model topology of the AFS configuration developed in Aspen Plus® is shown in Fig 7. The stripper component of the AFS was implemented in Aspen Plus® using the Radfrac block while each of the heat exchangers was represented with two heat blocks connected by a heat stream. The Radfrac block was simulated with 20 stages, with stages 1 to 19 representing the packed section and stage 20 representing the flash tank. The solvent hold-up and the residence time in the last stage were set to be lower than the rest of the stages to minimize solvent degradation.

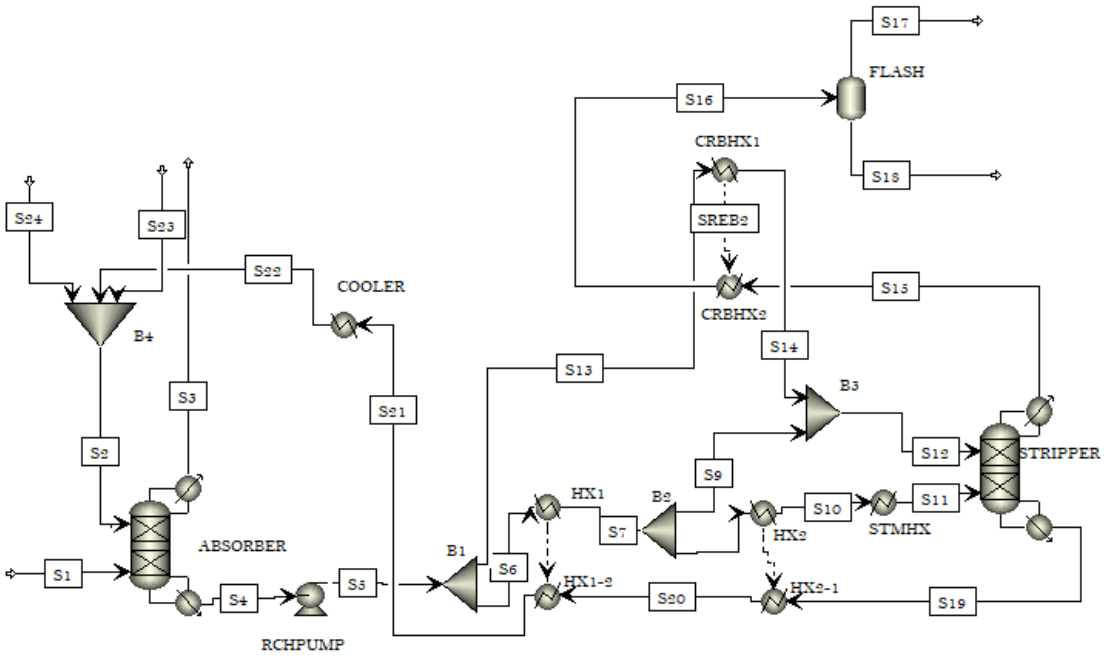

Fig 7. Advanced flash stripper model topology in Aspen Plus®

4.2. PCC process comparison using 30 wt% PZ vs 30 wt% MEA

PCC process with 30 wt% MEA is considered as the baseline to which other PCC processes are compared. The key parameters of the standard PCC process using 30 wt% PZ developed in this study are compared to the standard PCC process using 30 wt% MEA developed by Canepa et al.

[7] for the same NGCC power plant. It is important to state here that the type of packing used in the absorber and stripper in this study is different from the type of packing used in the absorber and stripper of the capture process developed by Canepa et al. [7]. This is because;

(1) The random packing used by Canepa et al. [7] is prone to the maldistribution of liquid and vapour phases in large diameter columns [67].
(2) Structured packings such as Mellapak 2X used in this study are regarded as appropriate packings for large-scale application [68,69].

The impact of lean loading on the regeneration energy for the standard PCC process using 30 wt% PZ is shown in Fig 8. The optimal lean loading is 0.2 mol_{CO2}/mol_{PZ}. This corresponds to the lowest regeneration energy of 3.2 GJ/t_{CO2}. Other results obtained from the simulations are compared to the 30 wt% MEA process in Fig. 9. The lean loading for the MEA process is 0.30 mol_{CO2}/mol_{MEA}. Due to the higher CO_2 capacity of the PZ solvent, the PCC process using 30 wt% PZ achieved a rich loading of 0.57 mol_{CO2}/mol_{PZ} against the value of 0.46 mol_{CO2}/mol_{MEA} achieved in the 30 wt% MEA process. This results in a 43% reduction in the solvent flow rate (405 kg/s) required by the PZ process. The L/G ratio is 0.88 kg/kg for the PZ process and 2.02 kg/kg for the MEA process. This indicates less solvent entering the stripper and thus less energy requirement for solvent regeneration. Also, there is less energy demand for pumping and cooling as well as less dissipation of heat in the cross-heat exchanger.

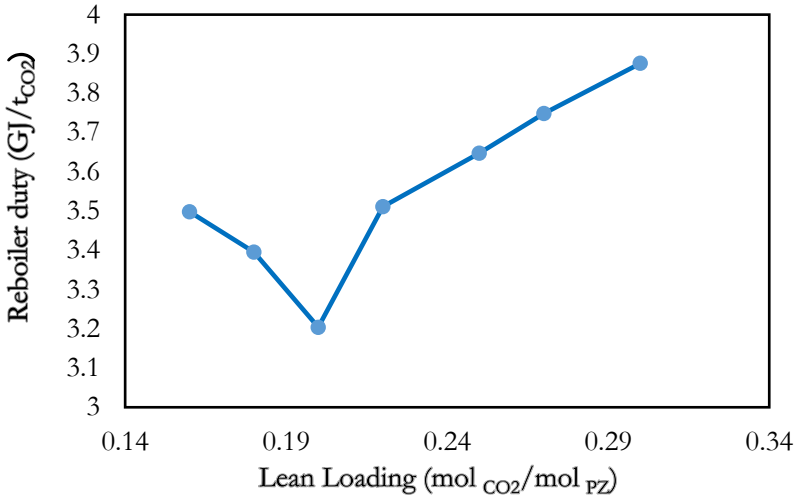

Fig 8. Impact of lean loading on the reboiler duty for the standard PCC process using 30 wt% PZ.

The PCC process using 30 wt% PZ also achieved lower specific energy consumption for solvent regeneration compared to the PCC process using 30 wt% MEA. The regeneration energy for the 30 wt% MEA process is 4.97 GJ/t_{CO2}. One reason for this high regeneration energy value is that the lean loading of 0.3 mol_{CO2}/mol_{MEA} used to design the MEA capture process in Canepa et al. [7] may not be the optimum lean loading, so the regeneration energy value could be reduced with a lower lean loading. Compared to the PCC process using 30 wt% MEA, the regeneration energy reduced by 36% to 3.20 GJ/t_{CO2} for the PCC process using 30 wt% PZ. The low sensible heat of PZ and less PZ solvent flowrate into the stripper are essential to the low energy consumption.

The diameter of the absorber and stripper is 10.7% and 2.4% smaller for the PCC process using 30 wt% PZ compared to the PCC process using 30 wt% MEA. Likewise, the packing height in the absorber and stripper is also reduced by 33%. This is due to the combined effect of the higher absorption capacity of the PZ solvent compared to the MEA solvent [20], and the Mellapak 2X packing used in the absorber and the stripper. The Mellapak 2X is a high-efficiency structured packing that reduces the total packing height due to its lower height of the transfer unit. The lower

solvent flowrate and size of the columns of the PCC process using 30 wt% PZ will reduce the operating and capital costs.

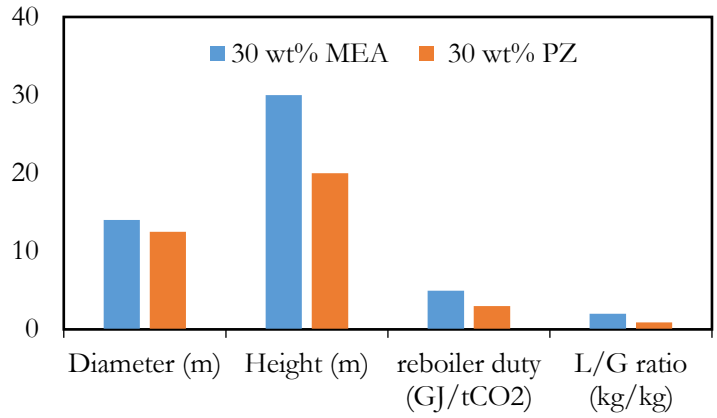

Fig. 9. Comparison of the PCC process performance between 30 wt% PZ and 30 wt% MEA for the standard PCC process.

5. Techno-economic performance assessment

5.1. Energy performance evaluation

The energy performance of the different configurations of the PCC process using different concentrations of PZ is evaluated based on the heat (steam) for the reboiler and the electrical energy to operate the pumps and the compressors. This represents the total energy required in (GJ) to capture and compress one tonne of CO_2. These energies have different exergy values and earlier work [70] suggested unifying them by converting the heat duty to equivalent work. This presents the heat duty on a similar basis as the pump and compression work and helps in determining how much electricity can be produced with the same amount of steam extracted from the steam turbine for solvent regeneration. In addition to the PCC process using PZ, the total equivalent work of a typical PCC process using the benchmark 30 wt% MEA solvent was evaluated. The equivalent work associated with the heat used for solvent regeneration was calculated using the Carnot efficiency method as shown in Eq. 16

$$W_{reg} = \eta_{turbine} Q_{reb} \left(\frac{T_{reb} + \Delta T - T_{sink}}{T_{reb} + \Delta T} \right) \quad 16$$

W_{reg} was calculated by assuming a turbine efficiency (η) of 76%, sink temperature (T_{sink}) of 313 K and steam side temperature approach (ΔT) of 10 K. Q_{reb} is the reboiler heat duty and T_{reb} is the reboiler temperature.

The total equivalent work is calculated from Eq. 17 as the sum of the regeneration heat work, compression work and pump work [71].

$$W_{eq} = \eta_{turbine} Q_{reb} \left(\frac{T_{reb} + \Delta T - T_{sink}}{T_{reb} + \Delta T} \right) + W_{comp} + W_{pump} \quad 17$$

The pump work is the total head required to move and circulate the solvent throughout the entire process. It includes the head to move the solvent from the absorber to the stripper pressure and to return it to the absorber. The values of the pump work (W_{pump}) was obtained directly from the Aspen Plus® simulation since it is one of the deliverables of the pump block in Aspen Plus®.

The work W_{comp} associated with the compression of the captured CO_2 from the stripper pressure to 150 bar in this work was obtained directly from the Aspen Plus® simulation. The compression train was simulated using the multistage compressor with four stages and coolers in-between them. The CO_2 was compressed from the stripper pressure of 1.65 bar to 150 bar and was cooled to 299.15 K in the last stage.

5.1.1. Energy performance results

Tables 7-9 show the performance of the different configurations and the contribution of the regeneration work *(W_{reg})*, compression work *(W_{comp})* and pump work *(W_{pump})* to the total equivalent work for each of the PZ concentrations. The calculated values of the total equivalent work were normalized by the tonnes of CO_2 captured. The standard PCC process with 30 wt% MEA has regeneration energy of 4.97 GJ/t_{CO2} and equivalent work of 5.34 GJ/t_{CO2}, which are the highest of all the configurations and solvent concentrations considered. Compared to the standard PCC process using 30 wt% MEA, the regeneration energy of the standard PCC process using PZ reduces by 35%, 41%, and 45% respectively for 30, 35 and 40 wt% PZ concentrations.

For the intercooling process configuration, the lowest regeneration energy of 2.61 GJ/t_{CO2} and lowest equivalent work of 2.96 GJ/t_{CO2} was achieved using 40 wt % PZ. These are 4% and 3.6% lower than the best results achieved for the regeneration energy and equivalent work with the standard configuration. The AFS with 40 wt% PZ has the lowest regeneration energy and equivalent work of 2.41 GJ/t_{CO2} and 2.76 GJ/t_{CO2} respectively among all the cases considered. Our regeneration energy values for the standard PCC process using 30 wt% PZ falls in the range of 3.4-4.0 GJ/t_{CO2} in Rochelle et al. [22], and those of the AFS are close to the value of 2.5 GJ/t_{CO2} reported in Gao et al.[6]. The two largest contributions to the total equivalent work are from the regeneration work and compression work, indicating that these two exact the highest energy penalty on the power plant for all the configurations.

Also, the cooling energy demands of the different configurations of the PCC process with various concentrations of PZ and standard PCC process using 30 wt% MEA are shown in Tables 7-9. With the standard configuration, the PCC process achieved the highest cooling energy demand of 2.10 GJ/t_{CO2} using 30 wt% MEA. Compared to the MEA process, the PCC process using PZ achieved a 9 %, 27% and 35% reduction in cooling energy demand when the PZ concentration was increased from 30-40 wt%. For the intercooling configuration, the cooling energy demand reduced from 1.80 GJ/t_{CO2} to 1.35 GJ/t_{CO2} (a 25% reduction) when the PZ concentration was increased from 30-40 wt%. The lowest cooling energy demand (1.35 GJ/t_{CO2}) for the intercooling configuration was obtained with a PZ concentration of 40 wt%. This represents a 0.7 % reduction in cooling demands compared to the best results obtained for the standard PCC process using PZ and a 36% reduction in cooling energy demand compared to the standard PCC process using 30 wt% MEA. The cooling energy demand of the AFS reduced by 14% when the PZ concentration was increased from 30-40 wt. The AFS achieved the lowest cooling energy demands of 1.09 GJ/t_{CO2} using 40 wt% PZ. This compared to the best results obtained with the standard and intercooling configurations represents a 20 and 19% improvement in cooling energy demand respectively. Compared to the standard PCC process using 30 wt% PZ, the AFS achieved a 48% reduction in cooling energy demands indicating that it has the best energy performance among the process configurations considered.

Table 7. Energy Performance of the standard PCC process configuration with 30 wt% MEA and different concentrations of PZ.

Solvent concentration	Optimum lean loading mol_{CO2}/mol_{amine}	Cooling (GJ/t_{CO2})	W_{reg} (GJ/t_{CO2})	W_{comp} (GJ/t_{CO2})	W_{pump} (GJ/t_{CO2})	W_{eq} (GJ/t_{CO2})
30 wt% MEA	0.30	2.10	4.97	0.37	0.003	5.34
30 wt% PZ	0.20	1.92	3.20	0.35	0.002	3.56
35 wt% PZ	0.20	1.52	2.93	0.35	0.001	3.28
40 wt% PZ	0.20	1.36	2.72	0.35	0.001	3.07

Table 8. Energy performance of the PCC process with Intercooling and different concentrations of PZ

Solvent concentration	Optimum lean loading mol_{CO2}/mol_{PZ}	Cooling (GJ/t_{CO2})	W_{reg} (GJ/t_{CO2})	W_{comp} (GJ/t_{CO2})	W_{pump} (GJ/t_{CO2})	W_{eq} (GJ/t_{CO2})
30 wt% PZ	0.20	1.80	3.05	0.35	0.002	3.41
35 wt% PZ	0.20	1.39	2.75	0.35	0.001	3.11
40 wt% PZ	0.20	1.35	2.61	0.35	0.001	2.96

Table 9. Energy performance of the PCC process with AFS and different concentrations of PZ

Solvent concentration	Optimum lean loading mol_{CO2}/mol_{PZ}	Cold rich bypass (%)	Warm rich bypass (%)	Cooling (GJ/t_{CO2})	W_{reg} (GJ/t_{CO2})	W_{comp} (GJ/t_{CO2})	W_{pump} (GJ/t_{CO2})	W_{eq} (GJ/t_{CO2})
30 wt% PZ	0.22	30	50	1.28	2.51	0.35	0.002	2.87
35 wt% PZ	0.22	30	50	1.16	2.45	0.35	0.002	2.81
40 wt% PZ	0.22	20	60	1.09	2.41	0.35	0.001	2.76

Table 10 shows the energy penalty on the NGCC power plant if it were integrated with the PCC process and compression unit. Here additional auxiliary power consumption for condenser pump, cooling water pumps, blower, and others which include the solvent make-up pumps, solvent filtration pumps, waste treatment pumps are added. The blower and pump power of the pre-treatment unit was taking from Canepa et al. [7]. The power required to operate each of the components listed in Table 10 except for the stripper is supplied in terms of electricity by the power plant. Therefore, the power loss of the power plant due to these components is directly obtained. On the other hand, steam is drawn from the power plant for solvent regeneration in the stripper. The electric power loss of the power plant associated with steam extraction was calculated using the method described in Linnenberg et al. [72]. The steam used in the stripper reboiler is at 130 °C and 3.9 bar. Therefore, the electric power loss due to solvent regeneration in Table 10 was calculated as the product of the extracted steam flow and power loss factor. The extracted steam flow is a product of the CO_2 capture level, reboiler duty, and mass flow of CO_2 in the flue gas. The power loss factor was calculated to be 0.195.

The NGCC power plant was not modelled in this work, therefore direct integration of the NGCC with the PCC plant was not done. The energy penalty in Table 10 was calculated with Eq. 18.

$$\text{Energy penalty} = \left(\frac{\text{Power output without Capture} - \text{Power output with capture}}{\text{Power output without capture}}\right)100 \quad 18$$

The power output with capture is the net power output of the power plant without capture minus the total power consumption of the PCC plant. Also, the efficiency penalty as shown in Table 10 was computed with Eq. 19.

$$\text{Efficiency penalty}(\%) = \text{Efficiency without capture} - \text{Efficiency with capture} \quad 19$$

In Table 10, the NGCC power plant has a net power output of 240 MW_e and a net electric efficiency of 53.34% without capture. With capture, the power plant achieves a net power output of 207.6 MW_e, 212.9MW_e, 214.4 MW_e, and 215.4 MW_e with standard PCC using 30 wt% MEA and 30-40 wt% PZ. These correspond to energy penalty of 10.24-13.5% and net efficiency fall from 53.5% to 46.3%, 47.4%, 47.8% and 48.1% for these processes. The highest efficiency penalty of 7.2% is achieved in the 30 wt% MEA process. The PCC process with absorber intercooling improves the net power output, energy penalty and efficiency penalty compared to the standard PCC process. The least efficiency penalty of 5.2% is achieved in the AFS with 40 wt% PZ.

The stripper reboiler heat duty shows to be the largest contributor to the total power consumption by the capture process followed by the CO_2 compression duty. The stripper reboiler duty accounted for 63% and the compression duty accounted for 27% of the total energy consumption with the standard PCC process using 30 wt% MEA. These values are in the range of 52-56% for reboiler heat duty and 33-36% for compression duty with the standard PCC process using PZ. With absorber intercooling, these values are in the range 51-54% for reboiler duty and 34-37% for compression duty. The stripper reboiler duty and the compression duty account for 49-50% and 37-38% of the total energy consumption respectively with the AFS using PZ.

Table 10. Energy consumption of the large-scale PCC process applied to an NGCC power plant

	NGCC									
	Without capture	**With standard capture**				**With PZ capture + absorber intercooler**			**With PZ capture + AFS**	
		30 wt% MEA	**30 wt% PZ**	**35 wt% PZ**	**40 wt% PZ**	**30 wt% PZ**	**35 wt% PZ**	**40 wt% PZ**	**30 wt% PZ**	**35 wt% PZ**	**40 wt% PZ**
Net Power Output (kWe)	240000	207599	212866	214402	215433	213299	214906	216050	216050	216113	216639
Net efficiency (%)	53.53[a]	46.31	47.48	47.83	48.05	47.57	47.93	48.19	48.19	48.20	48.32
Pre-treatment											
Blower duty (kWe)	nil	1390	1390	1390	1390	1390	1390	1390	1390	1390	1390
Pump duty (kWe)	nil	21	21	21	21	21	21	21	21	21	21
CO_2 capture Unit											
Rich solvent Pump (kWe)	nil	75.03	75.03	58.02	37.52	55.02	45.02	45.02	55.02	45.02	45.02
Lean solvent Pump (kWe)	nil	20.7	18.51	16.3	15.1	15.01	15.01	15.01	11	11	11
Reboiler (kWth)	nil	20300	15200	13900	12900	14500	13100	12400	12200	12000	11500
Condenser Pump (kWe)	nil	0.3	0.19	0.19	0.19	0.19	0.19	0.19	nil	nil	nil
Intercooler Pump (kWe)	nil	nil	nil	nil	nil	280.11	335.14	170.07	335.14	335.14	335.14
CO_2 compression Unit											
Compressors (kWe)	nil	9004	9004	9004	9004	9004	9004	9004	9004	9004	9004
Auxiliary											
Pumps for cooling water (kWe)	nil	390	320	309	301	316	292	288	305	287.70	275.80
Others											
Filtration, Water and solvent Make-up Pumps (kWe)	nil	1200	1105.60	900	898.30	1120	892.10	875.30	832.50	793.40	778.90
Total power consumption (KWe)		32401	27134	25598	24567	26701	25094	24208	24153	23887	23361
Efficiency Penalty (%)		7.23	6.05	6.20	5.48	5.96	5.60	5.34	5.34	5.33	5.21
Energy penalty (%)		13.50	11.31	10.67	10.24	11.13	10.46	9.98	9.98	9.95	9.7

[a] was calculated using a fuel rate of 9.89 kg/s [7] and LHV of 47220 kJ/kg [73]

5.2 Economic evaluation

The economic analysis of the PCC process was conducted using the Aspen Economic Process Analyzer® (APEA) and the detailed process flowsheet shown in Figs. 1-3. APEA uses the bottom-up approach based on the detailed process flowsheet, material and energy balances and equipment parameters. The simulations developed in Aspen Plus® are exported to APEA and the unit operations are mapped appropriately to separate equipment cost models available within the Icarus Evaluation Engine. Then they are sized and design according to relevant design codes. The process stream splitters of the AFS do not represent any project component in APEA [74], therefore they were typically mapped as an item with zero cost during the mapping and sizing of the process equipment.

APEA calculates the individual and direct costs of the PCC process equipment such as the absorber, stripper, heat exchangers, pumps, compressors, from which the capital expenditure (CAPEX) of the PCC plant is calculated. The OPEX consists of the fixed operating and maintenance (O&M) costs and the variable operating and maintenance (O&M) costs. The fixed O&M cost is made up of the total maintenance cost, labour costs, administration cost, laboratory cost etc. The variable O&M cost is based mainly on solvent consumption and utility costs. The fixed O&M was assumed as 3% of the CAPEX [75]. The variable O&M cost was calculated by multiplying the amount of utilities such as cooling water, electricity, solvent make-up and water make-up obtained from the Aspen Plus® simulation with their unit price. The total electricity consumption was obtained by adding the electricity consumed by pumps, compressors and blower to the equivalent electrical power derived from steam for solvent regeneration.

The utility unit prices used in the economic evaluation are provided in Table 12. PZ solvent has a higher resistance to degradation compare to MEA, therefore solvent loss due to degradation would be considerably lower for PZ. Solvent loss value of between 0.3-2.4 kg/t_{CO2} was reported for MEA [76–78]. In this study, a nominal solvent loss value of 1.5 kg/t_{CO2} was chosen for the MEA process and 0.05 kg/t_{CO2} was chosen for the PZ process [38]. The default cost value in the APEA database for electricity was maintained for electricity costing.

Table 12. Unit price of process utilities used for costing

Description	Value
Cooling water utility cost ($/m^3)[a]	0.35
Make-up MEA cost ($/ton)[b]	1500
Make-up PZ cost ($/ton)[b]	8000
Make-up water cost ($/m^3)[a]	3.0
Electricity price ($/kW)	0.0775
Operating time per year (hour)	8000

[a] prices obtained from [37]. [b] prices obtained from Alibaba.com

The total annual cost of the PCC plant is the sum of the annual capital cost (ACC) and annual operating costs. The ACC was calculated by annualizing the CAPEX using Eq. 20 [79] and adding the results to the OPEX.

$$ACC = \frac{\text{CAPEX}}{((1+\text{i})^{\text{n}}-1)\Big/\text{i}(1+\text{i})^{\text{n}}} \qquad 20$$

Where *n* is the project life (*n=20*) and *i* is the interest rate (*i=10%*).

5.2.1 Economic evaluation results

Although the economic performance of the PCC process configurations and the different solvent concentrations in Table 10 were evaluated, only the results for each of the three process

configurations (i.e. standard, intercooling and AFS) that achieved the least CAPEX, total annual cost and CO_2 avoided costs are presented here. The best economic performance for each of the process configurations is achieved with 40 wt% PZ. The economic performance of the 30 wt% MEA process is also included as a baseline to which the economic performance of the PCC processes using 40 wt% PZ is compared. Table 13 shows the total direct equipment cost obtained from the APEA for the PCC plant. It can be seen that the cost of the absorber dominates for all the cases considered followed by the cost of the stripper and compressor.

Table 13. Direct equipment cost of the large-scale PCC plant using 30 wt% MEA and 40 wt% PZ solvents for NGCC power plant

	Standard configuration + 30 wt% MEA	Standard configuration + 40 wt% PZ	Absorber Intercooler + 40 wt% PZ	AFS +40 wt% PZ
Equipment	Direct cost (M$)	Direct cost (M$)	Direct cost (M$)	Direct cost (M$)
Absorber	25.20	14.70	12.63	12.63
Lean solvent pump	0.30	0.15	0.15	0.15
Compressor	5.34	5.37	5.37	5.37
Solvent storage vessel	0.65	0.45	0.45	0.47
Rich solvent pump	0.34	0.14	0.14	0.15
Flash separator	0.16	0.16	0.16	0.14
Condenser	0.36	0.32	0.29	0.23
Stripper reflux drum	0.87	0.87	0.87	N/A
Stripper Reboiler	0.75	0.62	0.56	N/A
Reflux pump	0.28	0.28	0.28	N/A
Stripper	9.52	6.15	4.63	4.13
Lean cooler	0.37	0.19	0.14	0.23
Main cross-heat exchanger	5.56	0.72	0.59	nil
Absorber Intercooler	N/A	N/A	0.11	0.12
Intercooler pump	N/A	N/A	0.13	0.25
Cold-cross exchanger	N/A	N/A	N/A	0.44
Hot-cross exchanger	N/A	N/A	N/A	0.34
Cold-rich exchanger	N/A	N/A	N/A	0.21
Steam heater	N/A	N/A	N/A	0.50
Flash Tank	N/A	N/A	N/A	0.39
Total direct cost (TDC)	49.68	30.10	26.46	25.75

Table 14 shows the CAPEX of the standard PCC process using 30 wt% MEA against different configurations of the PCC process using 40 wt% PZ. The CAPEX of the capture plant was calculated based on the cost breakdown adopted in [37]. Compared to the MEA process, the PCC processes using PZ have smaller diameter and packing height for both the absorber and the stripper. This resulted in a significant reduction in the CAPEX for the PZ processes. One major contributor to the higher CAPEX in the MEA process is the packing height of 30 m required to achieve 90% capture. In the PZ processes, the packing height in the absorber and stripper is 20 m for the standard process, 15 m for the intercooled process and 15 and 10 m respectively for the AFS processes. According to Table 14, the CAPEX for the 30 wt% MEA process is about double the CAPEX for the capture processes using 40 wt% PZ.

The intercooled process despite the addition of an absorber intercooler and a pump in the intercooling loop has lower CAPEX compared to the standard PCC process using 40 wt% PZ.

This is because as the solvent is withdrawn, cooled in the intercooler and returned to the absorber at a much lower temperature (35 °C), its CO_2 absorption capability is enhanced. The CO_2 loading of the rich solvent slightly increased from 0.61 to 0.64. This reduced the packing height and the corresponding packing volume required to achieve 90% CO_2 capture. The intercooling reduces the absorber packing height by 5m and the packing volume by 17% (from 2120 m^3 in the standard PCC process with 40 wt% PZ to 1764 m^3 in the intercooled PCC process). In terms of CAPEX, the absorber of the standard PCC process using PZ is $2.09 million higher than the absorber of the intercooled PCC process with PZ. This value is much higher than the $0.24 million costs of the intercooler and the pump added to the cost of the intercooled PCC process.

The AFS process using 40 wt% PZ has the lowest CAPEX amongst all the processes. Most of the savings in CAPEX in the AFS are tied to the stripper, condenser and steam heater. In the standard stripper, the hot CO_2 vapour exiting the top of the stripper is cooled to 25 °C in the condenser. This results in the loss of the sensible heat and latent heat of the excess water vapour and consequently lost in work. The overhead condenser and the cross heat exchangers have been identified as the two largest sources of lost work and are responsible for over 70% of the total lost work of regeneration [80]. This particularly makes the standard stripper less efficient compared to the AFS which uses the cold-rich exchanger to recover heat from the hot vapour thereby eliminating the lost work in the condenser. Therefore, a smaller size condenser is required by the AFS compared to the standard stripper. The condenser cost in the AFS reduces by $0.1 million compared to the value of $0.32 and $0.29 million in the standard and intercooled configurations respectively. Also, the AFS uses a steam heater instead of the standard reboiler. The cost of the steam heater in the AFS process is $0.50 million while the cost of the reboiler in the standard and intercooled PCC processes are $0.62 and $0.56 million respectively. This represents an increase of 19% and 11% in cost for these components.

Table 14. CAPEX of the large-scale PCC plant using 30 wt% MEA and 40 wt% PZ solvents for NGCC power plant

		Standard configuration using 30 wt% MEA (M$)	Standard configuration using 40 wt% PZ (M$)	Absorber Intercooler using 40 wt% PZ(M$)	AFS with 40 using PZ (M$)
Total direct cost TDC		49.68	30.10	26.46	25.75
Total indirect cost (TIC)	20% of TDC	9.93	6.01	5.30	5.15
Bare erected cost (BEC)	TDC+TIC	59.60	36.10	31.80	30.90
Engineering and contractor (EC)	27% of BEC	16.10	9.74	8.59	8.35
Engineering Procurement and construction (EPC)	127% of BEC	75.70	45.80	40.40	39.30
Process contingency (PC)	25% of BEC	14.90	9.02	7.96	7.73
Project contingency (PJC)	20% of EPC+5% of BEC	18.10	11.00	9.68	9.40
Total plant cost (TPC)	120% of EPC+30% of BEC	109	65.80	58.10	56.40
Owner's cost (OC)	15% of TPC	16.30	9.87	8.71	8.46
Total capital expenditure (CAPEX)	115% of TPC	125.35	75.67	66.82	64.86

It is also evident from Table 15 that there is also a reduction in the ACC, fixed O&M cost and variable O&M cost of the PCC process using 40 wt% PZ compared to the PCC process using 30 wt% MEA. The largest cost contribution to the variable O&M is from electricity. For all the processes, the variable O&M dominates the total annual cost. The least-cost values for the ACC, fixed O&M, variable O&M and total annual cost are achieved with the AFS process with 40 wt% PZ. The values of the CO_2 capture cost are also shown in Table 15. Due to the significant reduction in the CAPEX and the total annual cost of the PCC plant with 40 wt% PZ, the CO_2 capture cost reduced to 40, 37.71 and 34.65 $\$/t_{CO2}$ respectively. These values are 34%, 37% and 42% lower than the value of 61.13 $\$/t_{CO2}$ obtained for the standard PCC process using 30 wt% MEA.

Table 15. Summary of the economic performance of the large-scale PCC process with 30 wt% PZ and 40 wt% PZ

Description		Standard configuration using 30 wt% MEA	Standard configuration using 40 wt% PZ	Absorber Intercooler using 40 wt% PZ	AFS using 40 wt% PZ
CAPEX (M$)		125.35	75.67	66.82	64.86
ACC (M$/yr)		14.70	8.89	7.84	7.62
Fixed O&M (M$/yr)		3.75	2.27	2.00	1.95
Variable O&M (M$/yr)	Electricity	24.54	18.32	18.14	16.02
	Cooling water	0.42	0.22	0.30	0.13
	Water make-up	0.52	0.56	0.56	0.55
	Solvent make-up	0.88	0.31	0.31	0.31
Total annual cost (M$/yr)		44.81	30.60	29.15	26.58
CO_2 capture cost ($/ton$_{CO2}$)		61.13	40.00	37.71	34.65

6. Conclusions

In this study, a rate-based model for the PCC process using PZ was developed in Aspen Plus®. The model was validated at pilot scale using experimental data from the literature. The validated model for the PCC plant was scaled up to process flue gas from a 250 MW_e NGCC power plant.

Technical analysis was performed to evaluate which process is most suitable for PCC. Technical analysis results show that the total energy demand of the PCC process reduces from 5.34 GJ/t_{CO2} with 30 wt% MEA to 3.56 GJ/t_{CO2} with 30 wt% PZ. The minimum energy demand of 2.76 GJ/t_{CO2} and minimum efficiency penalty of 5.32% was achieved with the AFS process using 40 wt% PZ.

The economic analysis was performed in Aspen Process Economic Analyzer® V8.4 and the results are presented in terms of the total annual cost and the CO_2 capture cost of the PCC process. The economic results show that the total annual cost of the standard PCC process with 30 wt% MEA and 40 wt% PZ are M$44.81/year and M$30.60/year respectively. The lowest total annual cost (M$26.58/year) and the lowest CO_2 capture cost ($34.65/tonne$_{CO2}$) were obtained using the AFS with 40 wt% PZ.

As the first detailed study on the technical and economic performance assessment of a large-scale PZ-based PCC process, this paper gained insights into the energy and cost requirements of the process. The results obtained can be helpful to policymakers when considering the large-scale deployment of the PZ-based PCC process

Acknowledgement

The first author is grateful to the Petroleum Technology Development Fund (PTDF), Nigeria (Ref: PTDF/ED/PHD/OOS/1086/17) for providing financial support to this study. The authors would like to acknowledge financial support from UK EPSRC under the grant of *UK Carbon Capture and Storage Research Centre 2017* (Ref: EP/P026214/1).

Appendix

A. Comparison of the open loop model predictions to the closed-loop model predictions.

In order to further demonstrates the superiority of the closed-loop model to the open-loop model, we have included the results obtained from the open-loop and the closed-loop simulation of two of the cases (3 and 5) used for model validation in section 3.2 in Table A1.

Table A1. Comparison of the open-loop model predictions to the closed-loop model predictions

	Exp.	OLM	RE (%)	CLM	RE (%)	Exp.	OLM	RE (%)	CLM	RE (%)
CO_2 capture level (%)	87.9	95	8.08	87.5	0.46	68.2	72	5.57	68.9	1.03
Lean loading (mol_{CO2}/mol_{PZ})	0.51	0.48	5.88	0.51	0	0.57	0.53	7.02	0.56	1.75
Rich loading (mol_{CO2}/mol_{PZ})	0.66	0.68	3.03	0.67	1.52	0.72	0.75	4.17	0.72	0
Captured CO_2 rate (kg/s)	0.036	0.039	8.33	0.0354	1.67	0.028	0.029	3.57	0.0283	1.07
Reboiler duty (MJ/kg_{CO2})	4.32	3.98	7.69	4.39	1.69	3.97	3.83	3.45	3.93	1.06
ARE (%)			6.60		1.07	ARE (%)		4.76		0.98

OLM= Open loop model, CLM= Closed-loop model, RE= Relative error, ARE=Average relative error.

B. Simulation (streams) results

Table B1. Results for material and energy flow flowrates in each stream of Fig.7

	S1	**S2**	**S3**	**S4**	**S5**	**S6**	**S7**	**S8**	**S9**	**S10**	**S11**	**S12**	**S13**	**S14**	**S15**	**S16**	**S17**	**S18**	**S19**	**S20**	**S21**	**S22**	**S23**	**S24**
T (K)	313.1	312	323.3	316	320	320	371	371	371	389	393	370	320	368	368	356	298	298	387	368	331	312	312	312
P (bar)	1.033	1.42	1.00	1.01	2.00	2.00	2.00	2.00	2.00	2.00	1.79	2.00	2.00	2.00	1.65	1.65	1.65	1.65	1.65	1.42	1.42	1.42	2.0	2.00
Vap. Frac	0.999	0	1	0	0	0	0	0	0	0.08	0.47	0	0	0	1	0.83	1	0	0	0	0	0	0	0
Mole Flow (kmol/)	12.63	10.9	12.53	10.5	10.5	8.40	8.40	3.36	5.04	3.42	3.54	7.14	2.10	2.10	0.98	0.97	0.56	0.41	10.08	10.08	10.08	10.08	0.85	0.023
Mass Flow (kg/s)	356	304.9	341	319.9	319.9	255.9	255.9	102	154	102	102	217.5	64	64	32.3	32.3	24.4	7.93	287.6	287.6	287.6	287.6	15.3	2.01
Volume Flow (cum/s)	317.6	0.321	338.8	0.302	0.301	0.241	0.25	0.1	0.15	4.29	30.0	0.212	0.06	0.06	18.3	14.7	8.50	0.01	0.323	0.316	0.307	0.303	0.02	0.003
Enth (Gcal/h)	-397	-2508	-295	-2621	-2621	-2097	-2069	-827	-1241	-812	-757	-1759	-524	-518	-272	-279	-188	-102	-2243	-2259	-2286	-2300	-207	-0.6
Mass Flow (kg/s)																								
PZ	0	74.9	1.64	19.5	15.0	12.0	17.2	6.89	10.3	13.6	27	14.6	3.0	4.22	0.4	0.02	0	0	82.4	78.7	74.9	73.3	0	2.0
H2O	16.7	172	24.4	163	165	132	132	52.6	78.9	52.6	53	112	33	32.9	7.6	7.5	0.2	7.4	157	157	157	157	15	0
CO2	27.06	0	2.71	0.01	0.00	0.00	0.02	0.01	0.01	2.74	7.9	0.02	0	0.00	24	24	24	0.0	0.01	0.00	0	0	0	0
H3O+	0	0	0	0	0	0	0	0	0	0	0	0	0	0	0	0	0	0	0	0	0	0	0	0
OH-	0	0	0	0	0	0	0	0	0	0	0	0	0	0	0	0	0	0	0	0	0	0	0	0
HCO3-	0	0.1	0	2.7	0.3	0.2	0.9	0.4	0.6	0.4	0.2	0.8	0.1	0.2	0	0.1	0	0.1	0.5	0.6	0.2	0.1	0	0
CO3-2	0	0.24	0	1.99	0.28	0.2	0.13	0.1	0.1	0	0.0	0.12	0.1	0	0	0.0	0	0	0.02	0.12	0.22	0.2	0	0
PZH+	0	21	0	31	46	37	30	12	18	9.3	3.1	26	9.2	7.6	0	0.1	0	0.1	8.5	16	19	21	0	0
PZH+2	0	0	0	0	0	0	0	0	0	0	0	0	0	0	0	0	0	0	0	0	0	0	0	0
HPZCOO	0	9.3-	0	71	44	35	45	18	27	14	8.1	38	8.8	11	0	0.3	0	0.4	28	17	12	9.7	0	0
$PZCOO^-$	0	20	0	30	16	12	8.5	3.4	5.1	3.3	2.1	7.3	3.1	2.2	0	0	0	0	12	12	17	19	0	0
$PZCOO^{-2}$	0	6.5	0	0.3	34	27	22	8.9	13	6.3	1.5	19	6.8	5.7	0	0	0	0	0	6.2	6.8	6.8	0	0
N2	307	0	307	0	0	0	0	0	0	0	0	0	0	0	0	0	0	0	0	0	0	0	0	0
AR	5.34	0	5.34	0	0	0	0	0	0	0	0	0	0	0	0	0	0	0	0	0	0	0	0	0

Table B2. Results for mass fraction and mole flowrate of components in each stream of Fig.7

Mass Fraction																								
	S1	**S2**	**S3**	**S4**	**S5**	**S6**	**S7**	**S8**	**S9**	**S10**	**S11**	**S12**	**S13**	**S14**	**S15**	**S16**	**S17**	**S18**	**S19**	**S20**	**S21**	**S22**	**S23**	**S24**
PZ	0	0.2	0.01	0.06	0.05	0.05	0.1	0.07	0.07	0.13	0.26	0.07	0.05	0.07	0.0	0	0	0	0.3	0.27	0.3	0.26	0	1
H2O	0.05	0.6	0.07	0.51	0.51	0.51	0.5	0.51	0.51	0.51	0.51	0.51	0.51	0.51	0.2	0.2	0	0.9	0.6	0.55	0.6	0.55	1	0
CO2	0.08	0	0.01	0	0	0	0	0	0	0.02	0.08	0	0	0	0.8	0.8	1.0	0.0	0	0	0	0	0	0
H3O+	0	0	0	0	0	0	0	0	0	0	0	0	0	0	0	0	0	0	0	0	0	0	0	0
OH-	0	0	0	0	0	0	0	0	0	0	0	0	0	0	0	0	0	0	0	0	0	0	0	0
HCO3-	0	0	0	0.01	0	0	0	0.01	0.01	0.01	0	0.01	0	0	0	0	0	0	0	0	0	0	0	0
CO3-2	0	0	0	0.01	0	0	0	0.00	0.00	0	0	0	0	0	0	0	0	0	0	0	0	0	0	0
PZH+	0	0.1	0	0.09	0.14	0.14	0.1	0.12	0.12	0.09	0.03	0.12	0.14	0.12	0	0	0	0	0	0.05	0.0	0.07	0	0
PZH+2	0	0	0	0	0	0	0	0	0	0	0	0	0	0	0	0	0	0	0	0	0	0	0	0
HPZCOO	0	0	0	0.22	0.14	0.14	0.2	0.18	0.18	0.14	0.08	0.18	0.14	0.18	0	0.0	0	0.1	0.1	0.06	0.1	0.03	0	0
PZCOO-	0	0.1	0	0.10	0.05	0.05	0	0.03	0.03	0.03	0.02	0.03	0.05	0.03	0	0	0	0	0.1	0.04	0.1	0.07	0	0
PZCOO-2	0	0.02	0	0.00	0.11	0.11	0.1	0.09	0.09	0.06	0.01	0.09	0.11	0.09	0	0.0	0	0	0	0.02	0.02	0.02	0	0
N2	0.86	0	0.9	0	0	0	0	0	0	0	0	0	0	0	0	0	0	0	0	0	0	0	0	0
AR	0.02	0	0.02	0	0	0	0	0	0	0	0	0	0	0	0	0	0	0	0	0	0	0	0	0
Mole Flow (kmol/s)																								
PZ	0	0.9	0.02	0.23	0.17	0.14	0.2	0.08	0.12	0.16	0.31	0.17	0.04	0.05	0.0	0	0	0	0.9	0.91	0.9	0.85	0	0.023
H2O	0.93	9.6	1.36	9.07	9.13	7.31	7.3	2.92	4.38	2.92	2.92	6.20	1.83	1.82	0.4	0.4	0.0	0.4	8.7	8.71	8.7	8.72	0.9	0
CO2	0.62	0	0.06	0	0	0	0	0	0	0.06	0.18	0	0	0	0.6	0.6	0.6	0	0	0	0	0	0	0
H3O+	0	0	0	0	0	0	0	0	0	0	0	0	0	0	0	0	0	0	0	0	0	0	0	0
OH-	0	0	0	0	0	0	0	0	0	0	0	0	0	0	0	0	0	0	0	0	0	0	0	0
HCO3-	0	0	0	0.04	0.01	0.01	0	0.01	0.01	0.01	0	0.01	0	0.01	0		0	0	0	0.01	0	0	0	0
CO3-2	0	0.0	0	0.03	0.01	0.0	0.0	0.0	0.0	0.0	0	0.0	0.0	0.0	0	0	0	0	0	0.0	0.0	0.01	0	0
PZH+	0	0.2	0	0.35	0.53	0.42	0.4	0.14	0.21	0.11	0.04	0.30	0.11	0.09	0	0.0	0	0.0	0.1	0.18	0.2	0.24	0	0
PZH+2	0	0	0	0	0	0	0	0	0	0	0	0	0	0	0	0	0	0	0	0	0	0	0	0
HPZCOO	0	0.1	0	0.55	0.34	0.27	0.4	0.14	0.21	0.11	0.06	0.29	0.07	0.09	0	0	0	0	0.2	0.13	0.1	0.07	0	0
PZCOO-	0	0.2	0	0.24	0.12	0.10	0.1	0.03	0.04	0.03	0.02	0.06	0.02	0.02	0	0	0	0	0.1	0.1	0.1	0.15	0	0
PZCOO-2	0	0	0	0.002	0.197	0.158	0.13	0.052	0.078	0.037	0.009	0.111	0.039	0.033	0	0	0	0	0	0.036	0.04	0.039	0	0
N2	11	0	11	0	0	0	0	0	0	0	0	0	0	0	0	0	0	0	0	0	0	0	0	0
AR	0.134	0	0.133	0	0	0	0	0	0	0	0	0	0	0	0	0	0	0	0	0	0	0	0	0

References

[1] Wu X, Wang M, Liao P, Shen J, Li Y. Solvent-based post-combustion CO_2 capture for power plants : A critical review and perspective on dynamic modelling, system identification, process control and flexible operation. Appl Energy 2020;257:1–25.

[2] Diego ME, Bellas JM, Pourkashanian M. Techno-economic analysis of a hybrid CO_2 capture system for natural gas combined cycles with selective exhaust gas recirculation. Appl Energy 2018;215:778–91.

[3] Adams T, Mac Dowell N. Off-design point modelling of a 420 MW CCGT power plant integrated with an amine-based post-combustion CO_2 capture and compression process. Appl Energy 2016;178:681–702.

[4] Wang M, Lawal A, Stephenson P, Sidders J, Ramshaw C. Post-combustion CO_2 capture with chemical absorption: A state-of-the-art review. Chem Eng Res Des 2011;89:1609–24.

[5] Oh SY, Yun S, Kim JK. Process integration and design for maximizing energy efficiency of a coal-fired power plant integrated with amine-based CO_2 capture process. Appl Energy 2018;216:311–22.

[6] Gao T, Selinger JL, Rochelle GT. Demonstration of 99% CO_2 removal from coal flue gas by amine scrubbing. Int J Greenh Gas Control 2019;83:236–44.

[7] Canepa R, Wang M, Biliyok C, Satta A. Thermodynamic analysis of combined cycle gas turbine power plant with post-combustion CO_2 capture and exhaust gas recirculation. Proc Inst Mech Eng Part E J Process Mech Eng 2013;227:89–105.

[8] Zhang Y, Chen CC. Modelling CO_2 absorption and desorption by aqueous monoethanolamine solution with Aspen rate-based model. Energy Procedia 2013;37:1584–96.

[9] Alhajaj A, Mac Dowell N, Shah N. A techno-economic analysis of post-combustion CO_2 capture and compression applied to a combined cycle gas turbine: Part I. A parametric study of the key technical performance indicators. Int J Greenh Gas Control 2016;44:26–41.

[10] Frimpong RA, Nikolic H, Pelgen J, Ghorbanian M, Figueroa JD, Liu K. Evaluation of different solvent performance in a 0.7 MWe pilot-scale CO_2 capture unit. Chem Eng Res Des 2019;148:11–20.

[11] Wu X, Wang M, Shen J, Li Y, Lawal A, Lee KY. Reinforced coordinated control of coal-fired power plant retrofitted with solvent-based CO_2 capture using model predictive controls. Appl Energy 2019;238:495–515.

[12] Song C, Liu Q, Ji N, Deng S, Zhao J, Kitamura Y. Natural gas purification by heat pump assisted MEA absorption process. Appl Energy 2017;204:353–61.

[13] Rezazadeh F, Gale WF, Rochelle GT, Sachde D. Effectiveness of absorber intercooling for CO_2 absorption from natural gas-fired flue gases using monoethanolamine solvent. Int J Greenh Gas Control 2017;58:246–55.

[14] Oyenekan BA, Rochelle GT. Energy Performance of Stripper Configurations for CO_2 Capture by Aqueous Amines. Ind & Eng Chem Res 2005;45:2457–64.

[15] Steeneveldt R, Berger B, Torp TA. CO_2 Capture and Storage: Closing the Knowing-Doing

Gap. Chem Eng Res Des 2006;84:739–63.

[16] Knudsen JN, Andersen J, Jensen JN, Biede O. Evaluation of process upgrades and novel solvents for the post-combustion CO_2 capture process in pilot-scale. Energy Procedia 2011;4:1558–65.

[17] Pan M, Aziz F, Li B, Perry S, Zhang N, Bulatov I, et al. Application of optimal design methodologies in retrofitting natural gas combined cycle power plants with CO_2 capture. Appl Energy 2016;161:695–706.

[18] Zhang R, Zhang X, Yang Q, Yu H, Liang Z, Luo X. Analysis of the reduction of energy cost by using MEA-MDEA-PZ solvent for post-combustion carbon dioxide capture (PCC). Appl Energy 2017;205:1002–11.

[19] Rochelle G, Chen E, Freeman S, Van Wagener D, Xu Q, Voice A. Aqueous piperazine as the new standard for CO_2 capture technology. Chem Eng J 2011;171:725–33.

[20] Freeman SA, Dugas R, Van Wagener DH, Nguyen T, Rochelle GT. Carbon dioxide capture with concentrated, aqueous piperazine. Int J Greenh Gas Control 2010;4:119–24.

[21] Chen E, Zhang Y, Lin Y, Nielsen P, Rochelle G. Review of Recent Pilot Plant Activities with Concentrated Piperazine. Energy Procedia 2017;114:1110–27.

[22] Rochelle GT, Wu Y, Chen E, Akinpelumi K, Fischer KB, Gao T, et al. Pilot plant demonstration of piperazine with the advanced flash stripper. Int J Greenh Gas Control 2019;84:72–81.

[23] Rabensteiner M, Kinger G, Koller M, Gronald G, Hochenauer C. Investigation of carbon dioxide capture with aqueous piperazine on a post-combustion pilot plant-Part I: Energetic review of the process. Int J Greenh Gas Control 2015;39:79–90.

[24] Chen E, Zhang Y, Lin Y, Nielsen P, Rochelle G. Review of Recent Pilot Plant Activities with Concentrated Piperazine. Energy Procedia 2017;114:1110–27.

[25] Kim I, Svendsen HF. Heat of absorption of carbon dioxide (CO_2) in monoethanolamine (MEA) and 2-(aminoethyl)ethanolamine (AEEA) solutions. Ind Eng Chem Res 2007;46:5803–9.

[26] Frailie PT. Modelling of carbon dioxide absorption/stripping by aqueous methyldiethanolamine/piperazine. PhD Thesis, USA: University of Texas at Austin, 2014.

[27] Li L, Voice AK, Li H, Namjoshi O, Nguyen T, Du Y, et al. Amine blends using concentrated piperazine. Energy Procedia 2013;37:353–69.

[28] Nguyen T, Hilliard M, Rochelle GT. Amine volatility in CO_2 capture. Int J Greenh Gas Control 2010;4:707–15.

[29] Plaza JM, Rochelle GT. Modelling pilot plant results for CO_2 capture by aqueous piperazine. Energy Procedia 2011;4:1593–600.

[30] Van Wagener DH, Rochelle GT, Chen E. Modeling of pilot stripper results for CO_2 capture by aqueous piperazine. Int J Greenh Gas Control 2013;12:280–7.

[31] Rabensteiner M, Kinger G, Koller M, Gronald G, Hochenauer C. Investigation of carbon dioxide capture with aqueous piperazine on a post-combustion pilot plant - Part II:

Parameter study and emission measurement. Int J Greenh Gas Control 2015;37:471–80.

[32] Cousins A, Huang S, Cottrell A, Feron PHM, Eric C, Rochelle GT. Pilot-scale parametric evaluation of concentrated piperazine for CO_2 capture at an Australian coal-fired power station. Greenh Gases Sci Technol 2014;5:7–16.

[33] Gao T, Rochelle GT. CO_2 Absorption from Gas Turbine Flue Gas by Aqueous Piperazine with Intercooling. Ind Eng Chem Res 2020;59:7174–81.

[34] Madan T, Van Wagener DH, Chen E, Rochelle GT. Modelling pilot plant results for CO_2 stripping using piperazine in two-stage flash. Energy Procedia 2013;37:386–99.

[35] Lin YJ, Chen E, Rochelle GT. Pilot plant test of the advanced flash stripper for CO_2 capture. Faraday Discuss 2016;192:37–58.

[36] Schach MO, Schneider R, Schramm H, Repke JU. Techno-economic analysis of post-combustion processes for the capture of carbon dioxide from power plant flue gas. Ind Eng Chem Res 2010;49:2363–70.

[37] Li K, Leigh W, Feron P, Yu H, Tade M. Systematic study of aqueous monoethanolamine (MEA)-based CO2 capture process: Techno-economic assessment of the MEA process and its improvements. Appl Energy 2016;165:648–59.

[38] Manzolini G, Sanchez Fernandez E, Rezvani S, Macchi E, Goetheer ELV, Vlugt TJH. Economic assessment of novel amine-based CO_2 capture technologies integrated with power plants based on European Benchmarking Task Force methodology. Appl Energy 2015;138:546–58.

[39] Abu-Zahra MRM, Niederer JPM, Feron PHM, Versteeg GF. CO_2 capture from power plants. Part II. A parametric study of the economical performance based on mono-ethanolamine. Int J Greenh Gas Control 2007;1:135–42.

[40] Agbonghae EO, Hughes KJ, Ingham DB, Ma L, Pourkashanian M. Optimal process design of commercial-scale amine-based CO_2 capture plants. Ind Eng Chem Res 2014;53:14815–29.

[41] Moioli S, Pellegrini LA. Improved rate-based modelling of the process of CO_2 capture with PZ solution. Chem Eng Res Des 2015;93:611–20.

[42] Sachde D, Chen E, Rochelle GT. Modeling Pilot Plant Performance of an Absorber with Aqueous Piperazine. Energy Procedia 2013;37:1987–2001.

[43] Zhang Y, Sachde D, Chen E, Rochelle G. Modeling of absorber pilot plant performance for CO_2 capture with aqueous piperazine. Int J Greenh Gas Control 2017;64:300–13.

[44] Gaspar J, Fosbøl PL. Simulation and multivariable optimization of post-combustion capture using piperazine. Int J Greenh Gas Control 2016;49:227–38.

[45] Van Wagener DH, Rochelle GT, Chen E. Modeling of pilot stripper results for CO_2 capture by aqueous piperazine. Int J Greenh Gas Control 2013;12:280–7

[46] Biliyok C, Lawal A, Wang M, Seibert F. Dynamic modelling, validation and analysis of post-combustion chemical absorption CO_2 capture plant. Int J Greenh Gas Control 2012;9:428–45.

[47] Ermatchkov V, Pérez-Salado Kamps Á, Speyer D, Maurer G. Solubility of carbon dioxide in aqueous solutions of piperazine in the low gas loading region. J Chem Eng Data 2006;51:1788–96.

[48] Posey ML, Rochelle GT. A Thermodynamic Model of Methyldiethanolamine− CO_2 −H 2 S−Water. Ind Eng Chem Res 1997;36:3944–53.

[49] Hetzer HB, Robinson RA, Bates RG. Dissociation constants of piperazinium ion and related thermodynamic quantities from 0 to 50.deg. J Phys Chem 1967;72:2081–6.

[50] Ermatchkov V, Pérez-Salado Kamps Á, Maurer G. Chemical equilibrium constants for the formation of carbamates in (carbon dioxide + piperazine + water) from 1H-NMR-spectroscopy. J Chem Thermodyn 2003;35:1277–89.

[51] Pinsent BR., Pearson L, Roughton FW. The kinetics of combination of carbon dioxide with hydroxide ions. Trans Faraday Soc 1956:1512–20.

[52] Bishnoi S, Rochelle GT. Absorption of carbon dioxide into aqueous piperazine: reaction kinetics, mass transfer and solubility. Chem Eng Sci 2000;55:5531–43.

[53] Razi N, Svendsen HF, Bolland O. Validation of mass transfer correlations for CO_2 absorption with MEA using pilot data. Int J Greenh Gas Control 2013;19:478–91.

[54] Rackett HG. Equation of State for Saturated Liquids. J Chem Eng Data 1970;15:514–7. https://doi.org/10.1021/je60047a012.

[55] Soave G. Equilibrium constants from a modified Redlich-Kwong equation of state. Chem Eng Sci 1972;27:1197–203.

[56] Horvath AL. Handbook of aqueous electrolyte solutions: Physical properties, estimation and correlation methods. Chichester: Ellis Horwood; 1985.

[57] Bird RB, Stewart EW, Lightfoot NE. Transport Phenomena. 2nd Editio. New York: John Wiley & Sons, INC; 2007.

[58] Wilke CR, Chang P. Correlation of diffusion coefficients in dilute solutions. AIChE J 1955;1:264–70.

[59] Aspen Tech. Aspen Physical Properties System - Physical Property Methods. available online. http://support.aspentech.com/ (accessed August 20, 2020).

[60] Hanley B, Chen C-C. New Mass-Transfer Correlations for Packed Towers. AICHE J 2012;58:2290–2.

[61] Chilton TH, Colburn AP. Mass Transfer (Absorption) Coefficients: Prediction from Data on Heat Transfer and Fluid Friction. Ind Eng Chem 1934;26:1183–7.

[62] Bravo JL, Patwardhan AA, Edgar TF. Influence of Effective Interfacial Areas in the Operation and Control of Packed Distillation Columns. Ind Eng Chem Res 1992;31:604–8.

[63] Van Wagener DH. Stripper Modeling for CO_2 Removal Using Monoethanolamine and Piperazine Solvents. PhD Thesis, USA: University of Texas at Austin, 2011.

[64] Otitoju O, Oko E, Wang M. A new method for scale-up of solvent-based post-combustion carbon capture process with packed columns. Int J Greenh Gas Control 2020;93:102900.

[65] Freeman SA, Rochelle GT. Density and viscosity of aqueous (piperazine + carbon dioxide) solutions. J Chem Eng Data 2011;56:574–81.

[66] Mazari SA, Ali BS, Jan BM, Saeed IM. Degradation study of piperazine, its blends and structural analogs for CO_2 capture: A review. Int J Greenh Gas Control 2014;31:214–28.

[67] Hoek PJ. Large and small scale liquid maldistribution in a packed column. PhD Thesis, Netherlands: Delft University of Technology, 1983.

[68] IEAGHG. CO_2 capture at gas-fired power plants. 2012/8: 2012.

[69] Luo X, Wang M. Improving Prediction Accuracy of a Rate-Based Model of an MEA-Based Carbon Capture Process for Large-Scale Commercial Deployment. Engineering 2017;3:232–43.

[70] Oyenekan AB, Rochelle TG. Alternative Stripper Configurations for CO_2 Capture by Aqueous Amines. AIChE J 2007;53:3144–54.

[71] Lin Y-J, Rochelle GT. Optimization of Advanced Flash Stripper for CO_2 Capture using Piperazine. Energy Procedia 2014;63:1504–13.

[72] Linnenberg S, Liebenthal U, Oexmann J, Kather A. Derivation of power loss factors to evaluate the impact of post-combustion CO_2 capture processes on steam power plant performance. Energy Procedia 2011;4:1385–94.

[73] NETL. Current and Future Technologies for Natural Gas Combined Cycle (NGCC) Power Plants. Natl Energy Technol Lab 2013:15–223.

[74] Aspen Technology Inc. Aspen Capital Cost Estimator: User's Guide. Aspen Technol Inc 2012; Version 8.:738.

[75] Luo X. Modelling, Simulation and Optimisation of Natural Gas Combined Cycle Power Plant Integrated with Carbon Capture. PhD Thesis, UK: University of Hull, 2016.

[76] Knudsen JN, Jensen JN, Vilhelmsen PJ, Biede O. Experience with CO_2 capture from coal flue gas in pilot-scale: Testing of different amine solvents. Energy Procedia 2009;1:783–90.

[77] Lepaumier H, Da Silva EF, Einbu A, Grimstvedt A, Knudsen JN, Zahlsen K, et al. Comparison of MEA degradation in pilot-scale with lab-scale experiments. Energy Procedia 2011;4:1652–9.

[78] Moser P, Schmidt S, Sieder G, Garcia H, Stoffregen T. Performance of MEA in a long-term test at the post-combustion capture pilot plant in Niederaussem. Int J Greenh Gas Control 2011;5:620–7.

[79] Karimi M, Hillestad M, Svendsen HF. Capital costs and energy considerations of different alternative stripper configurations for post-combustion CO_2 capture. Chem Eng Res Des 2011;89:1229–36.

[80] Lin Y-J, Rochelle GT. Approaching a reversible stripping process for CO_2 capture. Chem Eng J 2016;283:1033–43.